Spatiotemporal Independent Component Analysis for Retinal Images

Eduardo S. Barriga, Marios S. Pattichis
University of New Mexico, ECE Department
Image and Video Processing and Comm. Lab (ivPCL)
Albuquerque, NM
sbarriga@ieee.org

M.D. Abramoff[1], D. Ts'o[2], R. Kardon[1], Y. Kwon[1], and P. Soliz[3]
[1]University of Iowa, Dept. of Ophthalmology.
[2]State University of New York, Syracuse.
[3]Vision Quest Biomedical, Albuquerque, NM.

***Abstract*— This paper presents a new Independent Component Analysis algorithm (ICA-P) for modeling and measuring physiological responses to optical stimulation from a new, non-invasive optical imaging device. The ICA-P algorithm uses prior information on the visual stimulus to provide improved detection performance. In comparison with other methods that were considered (JADE, Infomax, SOBI, ESD, and Fast-ICA), ICA-P is shown to achieve significantly improved performance in detecting the retinal response to visual stimuli. Results from simulations show that we can estimate retinal reflectance changes as small as 0.01% (-40 dB, 10 dB lower than the other considered methods).**

Keywords: Independent Component Analysis, Retinal Imaging.

I. INTRODUCTION

In the field of ophthalmology, visual field testing (perimetry) is the gold standard for detection and monitoring progression of diseases in the optic nerve. Perimetry is a functional test of the patient's vision, which is intended to detect defects on the visual field map. Unfortunately, perimetry remains a subjective test that requires the patient to make important judgments during the test that can be clouded by anxiety, fatigue, or lack of concentration. Additionally, the sensitivity of this test is poor. Investigators have found that over fifty percent loss of ganglion cells is necessary to detect loss of function with perimetry [1]. This results in poor repeatability in areas where functional damage is suspected.

An optical imaging device of retina function (OID-RF) has been developed in an attempt to improve the objectiveness of the test and the sensitivity for detection of damage and change over time [2]. The OID-RF measures physiological changes in the retina due to neural activity resulting from visual stimulation of the photoreceptors.

The resulting optical recordings (videos) from the functional imaging device are a mixture of the signal that reflects the neuronal activity (functional signal) and signals related to unknown background sources and noise. Unfortunately, measured changes in reflectance in response to the visual stimulus are on the order of 0.1% to 1.0% of the total reflected intensity level which makes the functional signal difficult to detect by standard methods since it is masked by the other signals that are present. This paper is based on the application of Independent Component Analysis, a statistical signal processing technique, on the data obtained from the OID-RF.

In most adaptive filtering applications, an input and an output to a system are provided and the task is to determine the mathematical properties of the filtering system [3]. In recent years, a group of researchers investigated problems where not only the system is unknown, but also little is known about the inputs (sources). This work led to the development of independent component analysis (ICA), a set of statistical signal and image processing tools and algorithms that try to solve the blind source separation problem.

ICA has been applied to many biological problems such as electroencephalography (EEG), data analysis [4] and electrocardiogram (ECG) data analysis [5]. ICA has also been applied to extract functional brain responses due to visual or motor stimuli using recordings from techniques such as fMRI [6] and fNIR [7]. Schiessl et al. applied ICA techniques to isolate changes on the brain cortex of a macaque monkey due to visual stimulation [8]. The authors of this work have applied ICA techniques [9-10] to isolate the changes produced in the cat and human retina due to visual stimulation. This paper extends our prior work by incorporating prior information into the ICA algorithm.

This paper is organized as follows: Section II presents a description of the OID-RF. In section III the ICA methods are discussed. Section IV presents the results of the comparison of the ICA methods using synthetic and live data. In section V, a discussion of the results is presented.

II. OPTICAL IMAGING DEVICE FOR RETINAL FUNCTION

A. *Biological Principles*

Traditionally, neuronal activity in the central nervous system including the retina has been recorded electrically [11]. Recently however, noninvasive optical recording of neuronal signals from the brain has become possible [12]. Natural changes in the optical properties of active brain tissue (referred to as "intrinsic signals") permit visualization of neuronal activity when the surface of brain tissue is directly imaged using sensitive CCD cameras.

In our case, the intrinsic signals refer to the change in the percent reflectance of illuminating (or interrogating) light occurring as a result of the change in the absorption coefficient due to the conversion of oxyhemoglobin to deoxyhemoglobin in response to the metabolic demands of active neurons. The interrogating light is band-restricted to wavelength(s) where the difference in absorption spectra between the oxyhemoglobin and deoxyhemoglobin molecule is the greatest, typically in the region of 580-700nm.

Other sources of the intrinsic signals include changes in the microcirculation and light scattering that are also dependent on neuronal activity. The intrinsic signals from the brain are usually very small (0.1 to 1.0% of the overall reflected light intensity). However, when properly imaged, they can have high spatial resolution (50 microns) corresponding to the areas of active neuronal activity.

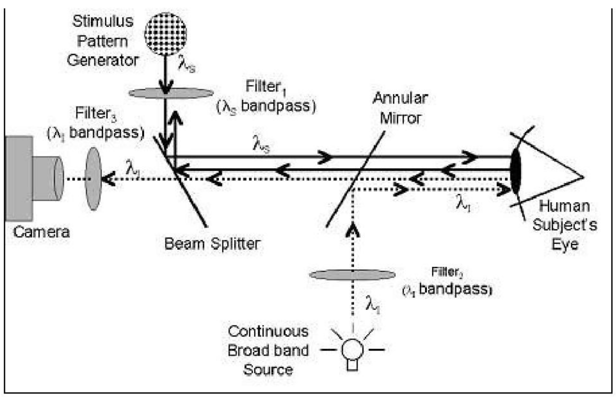

Figure 1. Optical pathway of the OID-RF

B. *OID Specifications*

The first OID-RF prototype was built using an existing commercial fundus camera and modifying the optical path by selectively filtering the continuous light source in the fundus camera to achieve an interrogation wave band. A stimulus pattern was presented at one wavelength (550nm), while interrogating the difference in reflectance due to oxyhemoglobin saturation change at a different wavelength (700 to 850 nm), using the same optical path. The 550 nm wavelength is called the stimulation wavelength, while the 700 to 850 nm wavelength is called the interrogation wavelength.

Fig. 1 shows a scheme of the optical array of the OID-RF. Band limited interrogation light source and a stimulus pattern in a different wavelength are projected to the retina. The reflected light from the retina is filtered by the beam splitter to only allow the interrogation light to pass through the CCD camera. The instrument was tested so that no light from the stimulus leaks into the camera. This would introduce false signals into the camera's field of view.

III. METHODS

A. *Independent Component Analysis*

Let $X = [x_1(t)\,x_2(t)\ldots x_n(t)]^T$ be a set of observed random variables and assume that they come from the linear mixture of the components $S = [s_1(t)\,s_2(t)\ldots s_n(t)]^T$ by a mixing matrix A, as in

$$X = A\,S. \tag{1}$$

Then independent component analysis consists of estimating both A and S using only the observations in X and the assumption that the source signals are statistically independent [5].

In this paper we present an ICA algorithm using prior information about the visual stimulus. This algorithm will be compared to three different ICA algorithms: Infomax [13]; which uses maximum likelihood estimation (MLE) to extract the sources that give the highest probability for the observations; JADE [14] a popular ICA algorithm that consists on using higher-order cumulant tensors; and SOBI [15] a method that incorporates time structure in the estimation of the sources.

B. *ICA Using Priors*

In the basic ICA model, no information is available about the original sources or the mixing matrix. But in many cases, some prior information about the system is known and it can be incorporated into the unmixing process. This will certainly be our case here since we know the onset and offset of the visual stimuli which indirectly gives us information about the mixing matrix. Calhoun et al. [6] used prior information on fMRI experiments to determine spatial locations and temporal information about the extracted sources.

For this work, a simplified version of Calhoun's algorithm was used. The Infomax algorithm is modified so that we incorporate prior information at each update cycle. The Bell-Sejnowski form of the Infomax algorithm is used, where the negative log-likelihood function for the unmixing matrix is given by:

$$f(W) = -\left[N\log|W| - \sum_{i,j}\cosh(WX) - NM\log(\pi)\right], \tag{2}$$

where N and M are the dimensions of the data. The gradient for this function is given by:

$$\Delta W = -\left[N\left(W^T\right)^{-1} - \tanh(WX)X^T\right]. \tag{3}$$

Using the log-likelihood function and the gradient we can use an optimization method to obtain an estimate of the mixing matrix. We used the BFGS method for unconstrained optimization. At each iteration, a normalized cross-correlation measure between the estimated mixing matrix and the prior of the mixing matrix is performed. If the correlation is lower than a tolerance value t then the estimated mixing matrix is updated as:

$$W^i = W^i + c\left(W_p^i - W^i\right) \quad (4)$$

where W^i is the i-th column of the estimated mixing matrix, W_p^i is the prior for that column and c is the confidence value (between 0 and 1) for the prior information. For $c = 0$ there will be no change in the estimated mixing matrix, while for $c = 1$ the estimated mixing matrix will be transformed completely into the prior.

IV. Simulation Results

In the ICA literature there have been many efforts to quantify the performance of the algorithms [16]. Most of these efforts are confined to one-dimensional data sets, with few focusing on 2-dimensional data and almost none on the three-dimensional video applications. It is therefore important to explore the performance of the selected ICA algorithms in realistic simulations of both general spatiotemporal data-sets as well as more specific data sets that are constructed from actual optical imaging data from the OID-RF device. In this section we present results from both a synthetic video simulation and a hybrid simulation using live data and synthetic stimuli.

A. *Synthetic Video Simulations*

A synthetic video is generated by mixing three images (sources) with a mixing matrix that contains the temporal structures of two sinusoids and a smoothed negative step function.

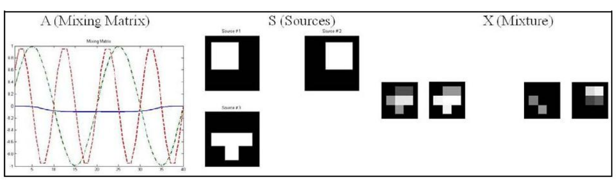

Figure 2. Experimental setup for the synthetic video simulation: Mixing matrix (left), sources (middle), and mixtures (right)..

1) *Experimental Setup*

Fig. 2 gives a graphical scheme of the mixture of the signals. The mixing matrix contains the temporal signal with 40 samples each. The temporal signals are:

- Sinusoid #1: Period is 20 samples, peak-to-peak amplitude is 2 (units are arbitrary).
- Sinusoid #2: Period is 10 samples, peak-to-peak amplitude is 2.
- Smoothed negative rectangular function: This function is formed as a union of two. The amplitude of this signal varies in three different experiments: 10 %, 5%, and 1% of the peak-to-peak amplitude of the sources.

The spatial signals are three 16-by-16 pixels binary images. The bright regions in those images (middle of Fig. 3) have a value of 1. The bright regions in the images were designed in such a way that when the linear mixture is performed using the mixing matrix, all mixing possibilities are covered. There are three regions which contain one temporal signal, three regions which are a mixture of two temporal signals and one region which contains a mixture of all the temporal signals described before. In total there are 7 different regions plus the background. The spatial arrangement also covers all the possible combinations of spatial mixing: (i) Three regions with one signal each, (ii) three regions with a mixture of two signals each, (iii) one region with a mixture of all the signals, and (iv) the background where no signal except noise is present.

The resulting mixture is a video with 40 frames (number of time points in the mixing matrix) and 256 pixels each frame. The video is input to the ICA matrix in a matrix form and the results of the estimation should give us the temporal structure (in the estimated mixing matrix) and the spatial structure (in the estimated sources). Noise is also added in the simulations, ranging from 40dB to 0dB in 10dB intervals.

2) *Synthetic Video Results*

The results of the normalized cross-correlations between the estimated sources and estimated mixing matrices are shown in Figs. 3 and 4. The "temporal" results refer to the comparison of the columns of the mixing matrices while the "spatial" results refer to the comparison of the sources with their estimated counterparts.

Spatial results for the rectangular signal (Fig. 3) show an increase in the performance of the ICA-P compared to the regular Infomax algorithm, but it is still 10% less accurate than JADE, especially for the 10% and 5% signals in the 40 to 20dB range.

The ICA-P achieves the best results in the temporal estimation of the rectangular signal in the video simulations. Fig. 4 presents the plots for the temporal estimation of the rectangular signal and it is clear how ICA-P matches the performance of JADE for high SNR and greatly improves the performance for low levels of SNR. These levels are where we had the most difficulty estimating the rectangular signal, especially when the signal is 1% of the peak-to-peak amplitude of the sinusoids.

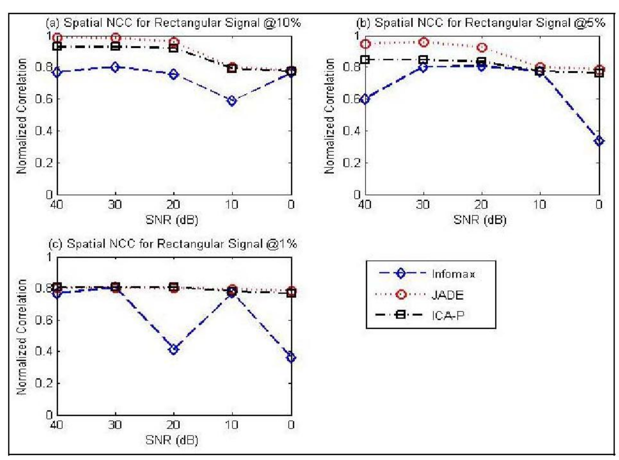

Figure 3. Spatial NCC results for the rectangular signal. Comparative results for JADE, Infomax, and ICA-P.

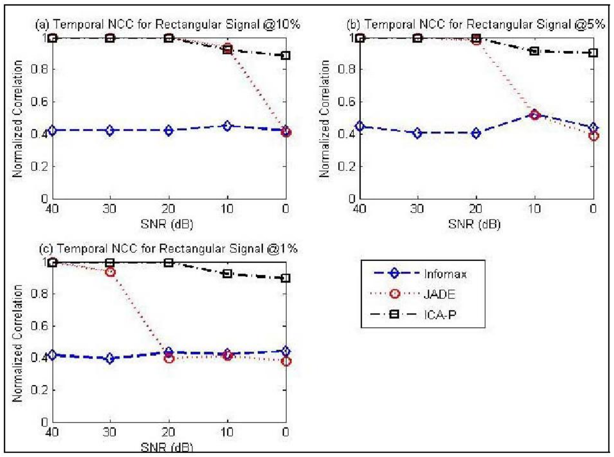

Figure 4. Temporal NCC results for the rectangular signal.

B. *Hybrid Simulations*

The next simulation involves both live data and synthetic stimulation. We use the OID-RF recordings from an unstimulated cat retina and add synthetic stimuli at different of levels of signal-to-background ratio (SBR). The synthetic stimuli are obtained from actual recordings of stimulated cat retina and synthesized so they can be easily manipulated in our simulation.

1) *Experimental Setup*

To synthesize the stimuli, we used a live cat experiment recording that presented a clear response and extracted a spatiotemporal profile of the response change during the experiment. The resulting "stimulation video" was then averaged and filtered to produce a smooth response and normalized to unit variance so it can be manipulated to produce the desired level of simulated response.

In the hybrid simulation no noise is added to the mixture. Instead, the amplitude of the stimulus is controlled by the signal-to-background ratio (SBR), defined as:

$$SBR(dB) = 10\log_{10}\frac{\sigma_S^2}{\sigma_B^2} \tag{5}$$

where σ_S^2 is the variance of the functional signal and σ_B^2 is the variance of the background.

Five videos were synthesized starting with the SBR ranging from 0 dB to -40 db at -10 dB intervals. Note that the more negative the SBR value, the lower the amplitude of the functional signal. A 0 dB SBR indicates that the variance of the functional signal is equal to the variance of the video, whereas a -30 dB SBR means that the variance of the functional signal is 0.1% of the variance of the video. Fig. 5 shows nine frames of a sample hybrid video at -20 dB SBR.

2) *Hybrid Simulation Results*

The results of the ICA algorithms were compared in the temporal and spatial domains. In the spatial domain, we correlated the sources as estimated by the ICA algorithms with a "reference frame," which is an image artificially generated by using a frame of pre-stimulated retina and the artificial stimulus

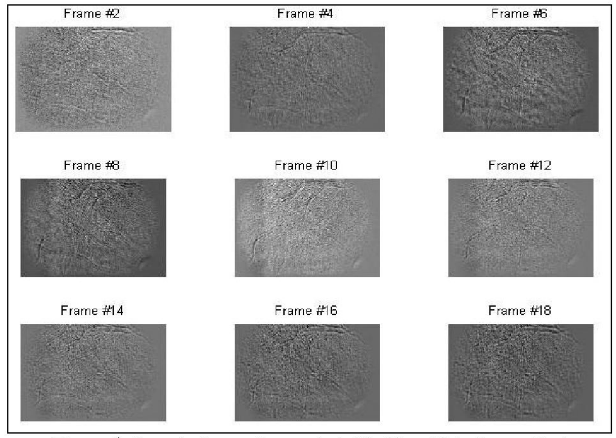

Figure 5. Sample frames from a hybrid video. Note the vertical synthetic stimulus on frames 8, 10, and 12.

response on top. For the temporal comparison, each row of the estimated mixing matrix was correlated with the modeled functional responses. A high correlation means that the estimated mixing matrix is following the time trace of the functional response expected due to visual stimulation.

The application of the ICA-P algorithm in the hybrid simulation yields similar results as with the synthetic video simulations. Increased NCC values are observed in the temporal cases (Figs. 6a and 6b) and a decrease compared to the Infomax in the spatial case (Fig. 6c). Note that the priors represent information about the *mixing matrix*. Therefore, in the *spatial domain*, it is somewhat expected that we increase the performance in the temporal domain and decrease it in the spatial domain. This is not a problem, since one of the most difficult parts in analyzing the data is recovering the correct temporal profile, and also we do not have (or use) priors in the spatial domain.

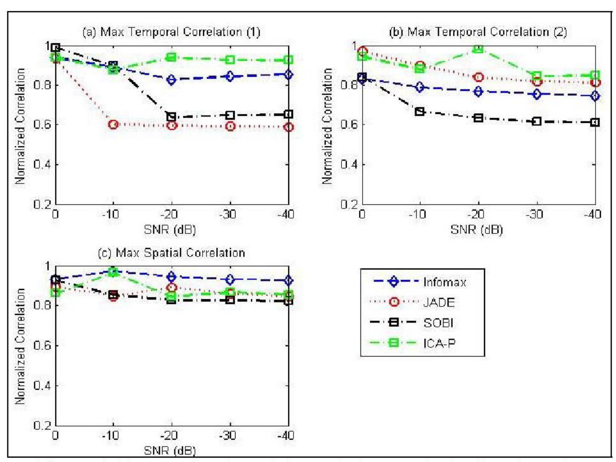

Figure 6. Temporal and spatial correlation results for live data plus synthetic stimulation experiments. (a) Temporal correlation results using the temporal reference 1. (b) Temporal correlation results using the temporal reference 2. (c) Spatial correlation results using the reference frame.

V. Discussion and Conclusions

The experiments have provided us with an improved understanding of the limits of what ICA algorithms can achieve, and how they can be improved. Our goal was to detect functional responses on the order of 0.1% (-30dB) of the total reflected signal. Our results showed how four ICA algorithms; JADE, Infomax, SOBI, and ICA-P produced estimates of the functional signals that were highly correlated with our reference signals.

For the performance of ICA-P in the 3-dimensional simulations, we note significant improvement over conventional ICA algorithms. The results of the temporal correlations for the synthetic video simulations (Fig. 5) showed an improvement of up to 30 dB in SNR while detecting the small (1%) rectangular signal when compared to the best performer of the conventional algorithms (JADE). The results on the hybrid simulations also showed an improvement in the temporal correlations of about 0.05 in absolute normalized cross-correlation. These results demonstrate the power of introducing prior information about the temporal structure of the experiments.

Significant improvement over the Infomax algorithm (in which the ICA-P is based) has been achieved in the synthetic simulations based on physiological data (Fig. 6). Moreover, the ICA-P outperformed conventional ICA algorithms for up to 30 dB, proving to be a powerful tool for the analysis of complex biological signals. In the problem of signal detection, the requirement was to estimate signals as small as 0.1% of the total intensity of the images, and we have achieved detection for signals as small as 0.01% (-40 dB SBR) in the hybrid data simulations.

Currently, the confidence and tolerance parameters are pre-specified and need to be chosen for each specific application. It is important to develop a way to automatically select the parameters that yield optimal performance of the ICA-P algorithm. Also, in addition to incorporating temporal prior information, it would be interesting to investigate ways of incorporating spatial priors to improve algorithmic performance. One of the main hurdles in this problem is the high dimensionality of the data in the case of spatial priors.

In conclusion, the analysis of the synthetic experiments has given us useful information in determining the threshold of stimulation that can be detected using the ICA algorithms. The analysis of these experiments should be applicable to any area where we have spatiotemporal mixing of the signals.

References

[1] H.A. Quigley, G.R. Dunkelberger, and W.R. Green, "Retinal ganglion cell atrophy correlated with automated perimetry in human eyes with glaucoma." Am J Ophthalmol, 1989. **107**: p. 453-464.

[2] R. Kardon, Y.H. Kwon, P.W. Truitt, S.C. Nemeth, D. Ts'o, and P. Soliz, "Optical imaging device of retinal function." in SPIE Photonics West. 2002. San Jose, CA.

[3] S. Haykin, "Adaptive Filter Theory." Prentice Hall Information and System Sciences Series. 2002, New Jersey.

[4] S. Makeig, A.J. Bell, T.-P. Jung, and T.J. Sejnowski, "Independent component analysis of electroencephalographic data," in Advances in Neural Information Processing Systems. 1996, MIT Press: Cambridge, MA. p. 145-151.

[5] A. Hyvarinen, J. Karhunen, E. Oja, "Independent component analysis." 2001, New York: John Wiley.

[6] V.D. Calhoun, and T. Adali, "Unmixing fMRI with Independent Component Analysis." IEEE Engineering in Medicine and Biology, 2006. **25**(2): p. 79-90.

[7] M. St. John, D.A. Kobus, J.G. Morrison, and D. Cshmorrow, "Overview of the DARPA Augmented Cognition Technical Integration Experiment." Intl Journal of Human-Computer Interaction, 2004. **17**(2): p. 131-149.

[8] I. Schiessl, M. Stetter, J.E. Mayhew, N. McLoughlin, J.S. Lund, and K. Obermayer, "Blind signal separation from optical imaging recordings with extended spatial decorrelation." IEEE Transactions on Biomedical Engineering, 2000. **47**: p. 573-577.

[9] E.S. Barriga, P.W. Truitt, M.S. Pattichis, D. Ts'o, Y.H. Kwon, R.H. Kardon, and P. Soliz, "Blind source separation in retinal videos." in The SPIE's International Symposium Medical Imaging 2003. 2003. San Diego, CA.

[10] E.S. Barriga, M.S. Pattichis, D.Y. Ts'o, Y. Kwon, R. Kardon, M.D. Abramoff, and P. Soliz, "Detection of low amplitude, in-vivo intrinsic signals from an optical imager of retinal function." in SPIE's Photonics West 2006. 2006. San Jose, CA.

[11] T.A. Berninger and G.B. Arden, "The pattern electroretinogram." Eye, 1988. **2**: p. S257.

[12] D.Y. Ts'o, R.D. Frostig, E.E. Lieke, and A. Grinvald, "Functional organization of primate visual cortex revealed by high resolution optical imaging." Science, 1990. **249**: p. 417-420.

[13] A.J. Bell and T.J. Sejnowski, "An information-maximization approach to blind separation and blind deconvolution." Neural Computation, 1995. **7**(6): p. 1003-1034

[14] J. Cardoso, "Infomax and maximum likelihood for blind source separation." IEEE Signal Processing Letters, 1997. **4**(4)..

[15] A. Belouchrani, K. Abed-Meraim, J. Cardoso, and E. Moulines, "A blind source separation technique using second-order statistics." IEEE Transactions on Signal Processing, 1997. **45**(2).

[16] A. Mansour, M. Kawamoto, and N. Ohnishi, "A survey of the performance indexes of ICA algorithms." in The IASTED International Conference Modeling, Identification and Control. 2002. Innsbruck, Austria).